Progress In Electromagnetics Research B, Vol. 46, 119–138, 2013

OBTAINING RAINDROP SIZE MODEL USING METHOD OF MOMENT AND ITS APPLICATIONS FOR SOUTH AFRICA RADIO SYSTEMS

Senzo J. Malinga and Pius A. Owolawi*

*Department of Electrical Engineering, Mangosuthu University of Technology, KwaZulu-Natal, South Africa

Abstract—In this paper, the Raindrop Size Distribution (DSD) modeling and analysis are presented. Drop sizes are classified into different rain types, namely: drizzle, widespread, shower and thunderstorm. The gamma and Lognormal distribution models are employed using the method of moments estimator, considering the third, fourth and sixth order moments. The results are compared with the existing raindrop size distribution models such as the three parameter lognormal distribution proposed by Ajayi and his colleagues and Singapore's modified gamma and Lognormal models. This is then followed by the implementation of the proposed raindrop size distribution models on the computation of the specific rain attenuation. Finally, the paper suggests a suitable raindrop size distribution model for the region with its expressions. The proposed models are very useful for the determination of rain attenuation for terrestrial and satellite systems.

1. INTRODUCTION

The quest for a huge bandwidth for higher data rates coupled with the congestion of lower frequencies has forced communication systems designers to explore the higher frequency bands. The higher frequencies such as microwave and millimeter waves are available and allow multi-Gbit/second signal transmission in terrestrial, satellite and wireless communications. The other advantages that are associated with the frequencies in this range are the immunity to interference, short range capacity coverage, frequency reuse, large bandwidth and easy deployment. At these higher frequencies, the propagation

Received 8 July 2012, Accepted 22 November 2012, Scheduled 25 November 2012
* Corresponding author: Pius Adewale Owolawi (p.owolawi@gmail.com).

attenuation due to environmental factors such as atmospheric gases, oxygen absorption, foliage blockage, scattering effect (diffused and specular reflection), fog, clouds and precipitation [1–5] is more pronounced. The chief contributor to impairment at these frequencies is the raindrop, which has roughly the same size as the radio wavelength at higher frequency, and thus causes scattering of the radio signal [3].

The microwave and millimeter wave attenuation depends considerably on rain rate and raindrop size distribution [3]. In view of the complexity of communication systems required to meet demands of today's users, the adequate knowledge of the rain characteristics of these bands is required in order to appropriately compensate for the signal loss [1–5].

In the field of Climatology, Meteorology, hydrology and radio communications, the spatial and temporal studies of rainfall characteristics such as rain rate and raindrop size distribution are important [6]. The reason lies in the unpredictability and stochastic behaviour of climatic parameters. Several researchers have solved this problem by employing empirical, analytical and statistical approaches [7–9]. The measurement of raindrop size distribution is very much a statistical process which depends on the data collected [7]. There are several measurement methods that have been used in the past for sampling the raindrop size distribution such as the filter paper method, the Doppler radar method, the Opto-electronic method and the electromechanical method. The latter is considered in this paper by using the Joss-Waldvogel RD-80 distrometer [7, 8]. The limitation of such equipment is in the spatial and temporal variation of raindrop size distribution. This limitation can be overcome through the use of radar equipment or employing advanced mathematical techniques to extrapolate point measurements by a Distrometer [1]. It should be noted that the most common reference available in calculating rain attenuation often uses rain intensity R, probably because of a scarcity of rain drop size data. The relationship between rain rate and drop size distribution $N(D)$ is given as :

$$R = 6\pi \times 10^{-4} \int_0^\infty D^3 v(D) N(D) dD \tag{1a}$$

where $v(D)$ represents the terminal velocity of raindrops in a still air and is measured in meters per second, and D is the equivalent spherical diameter in millimetres [9].

To account for the total attenuation at higher frequency in a system, the first step is to calculate the specific rain attenuation which depends on rain rate and the raindrop size. Extensive work in the South African context has been done by Owolawi [8] on rain rate distributions which are simply expressed by using a statistical distribution expression such as Power law, exponential distribution, gamma and lognormal distribution. In their recent contributions to the raindrop size distribution, it is observed that three popular distribution functions are used to describe raindrop size spectra. The Laws and Parsons [10] and Marshall and Palmer [11] are based on the exponential distribution, and generally used in temperate regions. The other two, Lognormal and modified gamma distributions, are peculiar to tropical and sub-tropical regions [12–16]. Researchers from Brazil [14], India [17], Malaysia [18], and Nigeria [19, 20], all from the tropical regions, have employed the latter two distribution functions to model the raindrop size for all kinds of rainfall characteristics in their respective regions. It has been established that the exponential method may not be suitable for tropical and sub-tropical regions, in which South Africa falls [7, 19].

The traditional modeling method with experimental DSD data is achieved by fitting the raw data which may result in large discrepancies between the modeled and the measured DSD data. The method of moments is often used to represent an estimated DSD input parameter.

The aim of the present work is to employ the method of moments to obtain the DSD parameters and apply the appropriate statistical distributions such as the Lognormal and modified Gamma functions. The results will be tested against the existing models and true DSD population spectra. The model parameters will then be further employed to determine the specific attenuation coefficients from 5 to 100 GHz using the proposed Lognormal models, attenuation cross-section that based on Mie scattering for different rain rate regimes.

2. EXPERIMENTAL SETUP AND DATA SORTING

In this work, the raindrop size distribution data is measured by the J-W RD-80 Distrometer. The equipment is capable of measuring raindrop diameters between 0.3 mm to > 5 mm with an accuracy of $\pm 5\%$. The equipment is positioned on the roof top of the School of Electrical, Electronics and Computer Engineering, Durban, South Africa. The geographical coordinates of where the equipment is positioned are latitude $29°52'S$ and longitude $30°58'E$, with an altitude of 139.7 meters above sea level. At this height, the windy conditions are taken into consideration. It is noted from many literature sources that windy condition serves as the largest single factor degrading measurement accuracy. It is often observed that small drops may pass the observing sensor area at low angles without falling in the sampling area. This

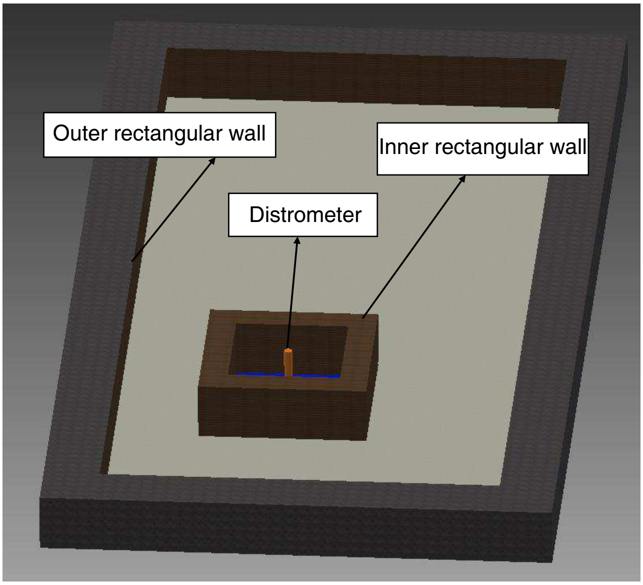

Figure 1. Distrometer enclosure on Durban site.

problem has led to false terminal velocity [21–25]. In order to minimize this problem, the Distrometer is placed within two rectangular wall enclosures as presented in Figure 1. Since the sampling area of a Distrometer is $50\,\mathrm{cm}^2$, the inner rectangular wall ($2\,\mathrm{m} \times 2\,\mathrm{m} \times 0.8\,\mathrm{m}$) is to prevent birds from damaging the cone part of the Distrometer and the outer rectangular wall ($3\,\mathrm{m} \times 4.14\,\mathrm{m} \times 11.6\,\mathrm{m}$) is to prevent the wind from drifting the rain drops away from reaching the sampling sensor area.

The data were collected over a period of two years and grouped into four rain regimes based on the rain rate and the general regime where all the raindrop size data is combined. The details of data sorting is described in reference [13]. Several authors have employed rain rate for the classification of raindrop size distribution into their respective rain types such as drizzle, widespread, shower and thunderstorm [20, 26–31]. As presented by Afullo [29], raindrop size is classified into the four classes based on the characteristic of unimodal and bimodal effects on the probability density of the drop size distribution in South Africa. Based on this reason, the same classes of rain rate classes are employed in this paper to categorize the raindrop size distribution into the following types:

- Drizzle ($0.1\,\mathrm{mm/hr} < R < 5\,\mathrm{mm/hr}$),
- Widespread ($5\,\mathrm{mm/hr} \leq R < 10\,\mathrm{mm/hr}$),

- Shower ($10\,\text{mm/hr} \leq R < 40\,\text{mm/hr}$),
- Thunderstorm ($R \geq 40\,\text{mm/hr}$).

It should be noted that the rain rate sampling rate is at 1-minute integration time as recommended by the ITU-R. The drop density decreases from drizzle to thunderstorm regime progressively, i.e., drizzle records over 46 000 samples while the thunderstorm sample number is less than 34.

3. DSD MODELS WITH THE METHOD OF MOMENTS (MOM)

In this section, two main statistical distributions are considered using the method of moments to describe the probability density distribution of the raindrop size data as classified in section one of the paper. The two distributions are the lognormal and modified gamma functions. The general expression to describe the rain rate, R, (in mm/hr) from the distrometer is given in [15]:

$$R = \sum_{i=1}^{20} \frac{3600\pi}{6ST} D_i^3 n_i \tag{1b}$$

where S is the area of the sensitive surface of the distrometer in m^2 ($S = 0.005\,\text{m}^2$), T the time interval for the measurements in seconds (the standard value of the $T = 60\,\text{s}$ was used), and ni the ith channel with diameter Di in mm. Note that the distrometer measured raindrop size distribution $N(D_i)(\text{m}^{-3}\text{mm}^{-1})$ based on the semi-empirical expression is:

$$N(D_i) = \frac{n_i \times 10^6}{v(D_i) \times S \times T \times \Delta D_i} \tag{2}$$

where n_i is the number of drops measured in drop size class i during the time interval T, ΔD_i the diameter interval of drop size class i, and $v(D_i)$ the terminal velocity of rain drop in (m/s) based on the Gunn and Kinzer expression [32]. The equivalent general model using any form of distribution function is summarized as in [13]:

$$N(D) = N_T \times pdf(D) \tag{3}$$

where N_T is the raindrop concentration per unit volume of rainfall drops for the different rain regimes and $pdf(D)$ the probability density function of the raindrop distribution. In this paper, we limit the discussion to the two distributions mentioned earlier to describe the $pdf(D)$. The advantages inherent in the application of MoM includes the simplicity of analytical application on the DSD parameters, and physical interpretation of the chosen function parameters of the DSD.

The statistical moment at nth order moment is theoretically expressed as [33]:

$$M_n = \int_{D\min}^{D\max} D_i^n N(D_i) dD = \sum_{i=1}^{20} D_i^n N(D_i) dD_i \tag{4}$$

where $D_{\max}$ and $D_{\min}$ are 5 mm and 0.3 mm for the J-W RD-80. To compute raindrop size distribution parameters from the distrometer, Equation (4) is employed and re-expressed as [34]:

$$M_n = \sum_{i=1}^{20} D_i^n \left[\frac{ni}{S \times T \times v(D_i)} \right] \quad \left[\mathrm{m}^{-3}\mathrm{mm}^n\right] \tag{5}$$

Equation (5) is applied to the distrometer measured data and the collected data are then equal to the statistical equivalent at the chosen order of the moment.

3.1. Gamma Distribution Model and MoM

In this study, J-W RD-80 distrometer data were fitted using a modified gamma distribution by employing an estimator method of moments. The modified gamma distribution technique is considered because of its ability to represent DSD parameters at low and high diameter of drops. The general expression for raindrop size distribution is given as [15, 29, 35]:

$$N(D_i) = f(D_i) N_T = N_o D_i^{\mu} \exp(-\Lambda D_i) \quad (\mathrm{m}^3/\mathrm{mm}) \tag{6a}$$

$$f(D) = C D^{\alpha-1} \exp \ [-D/\beta]$$
$$N_o = N_T C = N_T \frac{\Lambda^{\mu+1}}{\Gamma(\mu+1)}; \ \ \mu = \alpha - 1; \ \ \Lambda = \frac{1}{\beta} \tag{6b}$$

where the DSD parameters $N_o\,(\mathrm{mm}^{-1}\mathrm{m}^{-3})$, μ, and $\Lambda\,(\mathrm{mm}^{-1})$ are the intercept, shape and slope parameters respectively. Note that α is the shape parameter, β is the scale parameter, and C is a constant that depends on α and β as shown in Equation (6b) above. By equating M_n in Equation (5) to Equation (6), the resulting solution for the constants of the the modified gamma distribution considering the moment order $n = 3$, 4, and 6, as presented in [16], is:

$$\mu = \frac{11F - 8 + \sqrt{F(F+8)}}{2(1-F)} \tag{7}$$

where

$$F = \frac{M_4^3}{M_3^2 M_6} \quad \text{and} \quad \Lambda = (\mu + 4)\frac{M_3}{M_4} \tag{8}$$

$$N_o = \Lambda^{\mu+4}/\Gamma(\mu + 4) \tag{9}$$

In this paper, the statistical relationship between rain rate and DSD parameters are employed in order to explain the characteristics of raindrop size distributions as demonstrated by many authors in the past. Popular among them are, Marshall-Palmer [11], Ulbrich [35], Timothy et al. [36], Ajayi et al. [20], Fišer et al. [26] and Afullo [29]. These constants are computed with the available raindrop size distribution data to plot the scatter plots shown in Figure 2. For simplicity, the results are fitted with their respective suitable relationships as presented in Table 1. The same approach is applied to all the rain regimes and only the shower sample is presented as a sample. It is observed that the results produced weak correlation coefficients (R^2), hence the second distribution (Lognormal distribution) is considered and used in this paper due to the improvement in the value of the correlation coefficients. Based on the rain regimes discussed in Section 2 of this paper, the scatter plots for the shower rain type is presented in Figure 2. The summary of the fitted raindrop distribution parameters for gamma are presented in Table 1. The presence of different forms of relationships between rain rate and DSD parameter as presented in Table 1 may be due to secondary peaks/bimodal and shifts that present in the DSD spectral as confirmed by several authors [29, 40]. The type of relationships chosen are often used based on the best correlation coefficients by authors who had worked on the microphysics of DSD [15–38]. Based on these reasons stated earlier, the choice of different relationships between rain rate and DSD parameters is considered in fitting the DSD parameters.

It consists of a mix of power, logarithm, polynomial (2nd order) and linear relationships. It is noted that the raindrop counts are well represented by the power law while other parameters are fitted with different relationship types attaining the best correlation coefficients. The correlation coefficient in the gamma distribution is weak; this may be due to the clusters of the data used. It is observed in Figure 2 that the spread of variability of DSD parameters decreases as the rain rate progressively increases. The reduction in variability of DSD parameters observed may be as a result of a reduction in the DSD parameter range.

It should be noted that the relationship between R and different DSD parameters are fitted using the least-squares criterion, after the method of moments has been used to deduce the values of the DSD

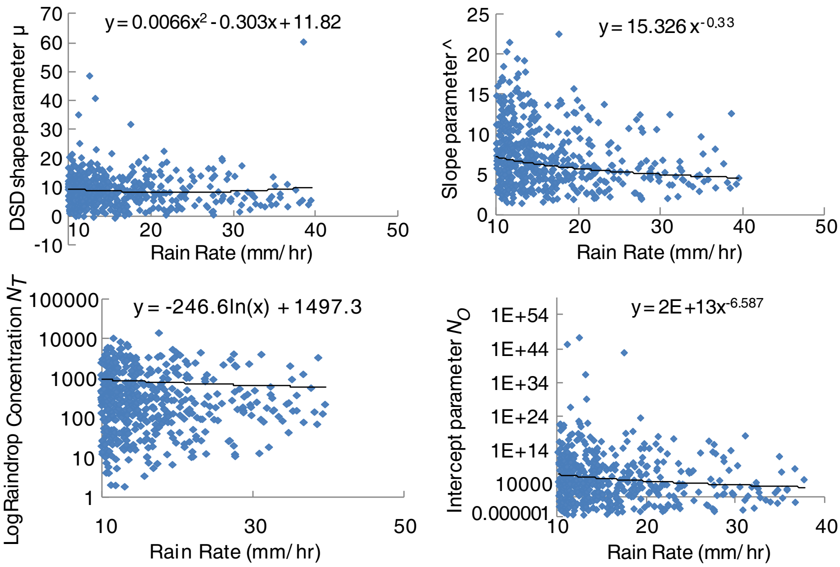

Figure 2. Scatter plots for shower: Gamma parameters against rain rate.

parameters from the raindrop size spectra, which take into account the third, fourth and sixth order moments.

3.2. Lognormal Distribution Model and MoM

The probability density function of the three-parameter lognormal distribution is considered with a little modification of the distribution input variables. The three-parameter lognormal distribution is expressed as:

$$N(D) = N_T \times pdf(D; \gamma, \mu, \sigma) \tag{10}$$

where the random variable mean droplet diameter, D, is said to have a three-parameter lognormal distribution if the random variable $Y = \ln(D - \gamma)$, where D is greater than γ, is normally distributed $(\mu,\ \sigma^2)$, and σ is considered to be greater than zero. The probability density function of the three-parameter lognormal distribution is then given by Pan et al. [37] as:

$$pdf(D; \gamma, \mu, \sigma) = \frac{1}{\sigma\sqrt{2\pi}(D-\gamma)} \exp \frac{-1}{2\sigma^2}[\ln(D-\gamma)-\mu]^2 \qquad \gamma < D < \infty \quad \sigma > 0 \tag{11}$$

Equation (10) will be zero if the conditions in Equation (11) are not met. Parameter σ^2 is the variance of Y; it defines the shape parameter

Table 1. Summary of gamma parameter model for raindrop size distribution in Durban.

Rain regime	Raindrop Count	Raindrop Concentration N_T
Thunderstorm	$531.39R^{0.0912}$ $R^2 = 0.013$	$639.31LN(R) - 1679$ $R^2 = 0.02$
Shower	$403.89R^{0.1}$ $R^2 = 0.09$	$-246.6LN(R) + 1497.3$ $R^2 = 0.03$
Widespread	$284.31R^{0.3317}$ $R^2 = 0.04$	$2 \times 10^{44}R - 2 \times 10^{44}$ $R^2 = 0.01$
Drizzle	$250.93R^{0.424}$ $R^2 = 0.016$	$10^{45}R - 3 \times 10^{44}$ $R^2 = 0.06$
General	$270.36R^{0.407}$ $R^2 = 0.4$	$-2 \times 10^{44}(LN(R) + 1)$ $R^2 = 0.59$
Rain regime	Intercept N_o	Slope parameter
Thunderstorm	$10^6R^{0.2727}$ $R^2 = 0.05$	$13.697R^{-0.316}$ $R^2 = 0.02$
Shower	$2 \times 10^{+13}R^{-6.587}$ $R^2 = 0.02$	$15.326R^{-0.33}$ $R^2 = 0.04$
Widespread	$6 \times 10^{58}(LN(R) - 1)$ $R^2 = 0.05$	$8 \times 10^{+12}LN(R)$ $-2 \times 10^{13}R^2 = 0.01$
Drizzle	$-6 \times 10^{29}LN(R)$ $+2 \times 10^{296}R^2 = 0.08$	$9 \times 10^{+13}LN(R)$ $-2 \times 10^{14}R^2 = 0.07$
General	$7 \times 10^{270}R^2 - 5 \times 10^{272}R$ $+3 \times 10^{273}R^2 = 0.35$	$-3 \times 10^{12}(LN(R) + 1)$ $R^2 = 0.46$
Rain regime	DSD slope parameter μ	
Thunderstorm	$0.0028R^2$+0.390R-5.7139 $R^2 = 0.07$	
Shower	$0.0066R^2 + 0.303R + 11.82$ $R^2 = 0.04$	
Widespread	$9 \times 10^{+12}LN(R) - 2 \times 10^{13}$ $R^2 = 0.01$	
Drizzle	$-2 \times 10^{15}R^2 + 8 \times 10^{14}R$ $-6 \times 10^{13}R^2 = 0.09$	
General	$2 \times 10^{10}R^2 - 10^{12}R - 10^{12}$ $R^2 = 0.63$	

of D, where μ is the mean of Y. The method of moments is considered with a condition that $\gamma = 0$, with an expression such that:

$$M_n = N_T \exp\left[n\mu + \frac{1}{2}(n\sigma)^2\right] \tag{12}$$

Using the same moment order as presented in the gamma distribution, the three input parameters are expressed as follows [38]:

$$N_T = \exp\left[(24L_3 - 27L_4 + 6L_6)/3\right] \tag{13}$$

$$\mu = \left[(-10L_3 + 13.5L_4 - 3.5L_6)/3\right] \tag{14}$$

$$\sigma^2 = \left[(2L_3 - 3L_4 + L_6)/3\right] \tag{15}$$

where L_3, L_4 and L_6 represent the natural logarithms of the measured moments M_3, M_4 and M_6 respectively. In the case of Lognormal distribution, the scatter plot for widespread rain is chosen and presented in Figure 3. The lognormal model parameters are fitted with different laws as with the case of the gamma distribution, the only change is in the correlation coefficients, which is better relative to the gamma distribution. Table 3 shows a summary of the fitted lognormal model parameters for different rain regimes.

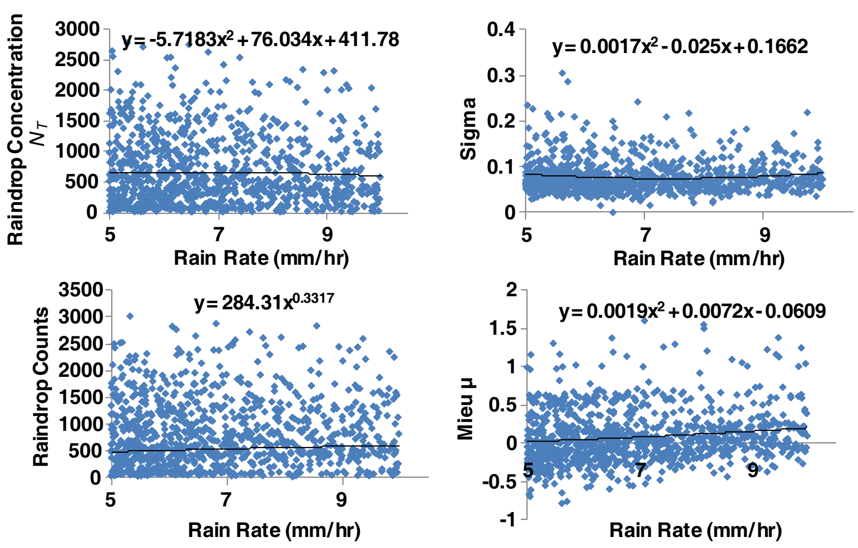

Figure 3. Scatter plots for widespread: Lognormal parameters against rain rate.

Table 2. Summary of lognormal parameter model for raindrop size distribution in Durban.

Rain regime	Raindrop Count	Raindrop Concentration N_T
Thunderstorm	$531.39R^{0.0912}$ $R^2 = 0.31$	$0.051R^2 - 4.0654$ $+662.28R^2 = 0.40$
Shower	$403.89R^{0.1}$ $R^2 = 0.14$	$-0.0619R^2 + 0.5595R$ $+518.44R^2 = 0.49$
Widespread	$284.31R^{0.3317}$ $R^2 = 0.39$	$-5.7183R^2 + 76.034R$ $+411.78R^2 = 0.70$
Drizzle	$250.93R^{0.424}$ $R^2 = 0.40$	$-856.82R^2 + 1381.5R$ $+33.89R^2 = 0.63$
General	$270.36R^{0.407}$ $R^2 = 0.60$	$221.45R^{0.354}$ $R^2 = 0.80$
Rain regime	**Mieu μ**	**Sigma σ**
Thunderstorm	$0.17R^{0.2727}$ $R^2 = 0.37$	$2 \times 10^{-5}R^2 - 0.003R$ $+0.1895R^2 = -0.59$
Shower	$0.0003R^2 + 0.0269R$ $+0.0034R^2 = 0.61$	$0.0644R^{0.0738}$ $R^2 = 0.62$
Widespread	$0.0017R^2 - 0.025R$ $+0.1662R^2 = 0.72$	$0.0019R^2 + 0.0072R$ $-0.0609R^2 = 0.78$
Drizzle	$-5.6587R2 + 3.22R$ $-0.8686R^2 = 0.70$	$-0.5759R^2 + 0.3181R$ $+0.0286R^2 = 0.72$
General	$0.1504\ln(R) - 0.2594$ $R^2 = 0.83$	$0.0088L_n(R) + 0.0742$ $R^2 = 0.87$

Table 3. RMSE for different raindrop size distribution models in percentage.

Rain Rate mm/hr	Lognormal Model West Africa	Lognormal Model Singapore	Modified Gamma Singapore	Proposed Lognormal Model	Proposed Gamma Model
5	7.99	11.89	9.05	3.72	9.14
10	9.23	14.90	12.19	4.21	11.15 v
25	10.85	19.49	19.55	4.72	13.92
100	13.73	28.33	52.73	6.38	17.94

4. COMPARATIVE STUDIES

The accuracy of the proposed models can be evaluated by performing the Root Mean Square Error (RMSE) test as a percentage. The performance technique is employed as prescribed and used by several authors who have worked in this area of study [15, 16, 28]. The expression is presented as:

$$\text{RMSE} = 100 \times \sqrt{\frac{1}{N}\sum_{i=1}^{N}[N(D_i) - \text{modelled}\, N(D_i)]^2} \tag{16}$$

where $N(D_i)$ is the calculated droplet size of the measured data, and N denotes the number of channels provided by the distrometer measurement system. The modeled $N(D_i)$ represents the proposed and existing models from other regions of the world. Although, the RMSE is used in this work because it is widely employed to describe the average model performance, nevertheless, it has been reported to be inappropriate and misinterpreted the measure of average error [43]. Figure 4 shows the measured DSD data and existing models like the modified gamma distribution model [38, 39] (Singapore model) and lognormal model [19] (proposed and west Africa model) and the proposed gamma model. Table 3 gives a summary of the percentage of RMSE for different rain rates and raindrop size distribution models. Table 3 shows that the RMSE ranges between 3.72% and 52.73%. The table reveals that as the rain rate increases, the RMSE increases progressively in all the compared models. The highest value of RMSE is recorded in the modified gamma model (Singapore) and the least RMSE is observed in the proposed lognormal model. Based on the RMSE, the best performance of the proposed and existing models are presented as follows: modified gamma model (Singapore), Lognormal model (Singapore), proposed gamma model, Lognormal model (West Africa) and proposed Lognormal model.

5. SPECIFIC RAIN ATTENUATION

In this paper, we used the Mie Scattering theory to calculate specific rain attenuation using local rain rate and drop size distribution data collected in Durban, South Africa. Since in this paper our interest is to study the characteristics of the specific attenuation in different rain classes, the adoption of the Mie Scattering has been considered. The polarization independent specific rain attenuation denoted by A_s (dB/km) is calculated by integrating the raindrop size distribution models and is given, as in [40, 41], by:

$$A_s = 4.343 \times 10^{-3} \int_0^\infty Q(D, \lambda, m) N(D) dD \tag{17}$$

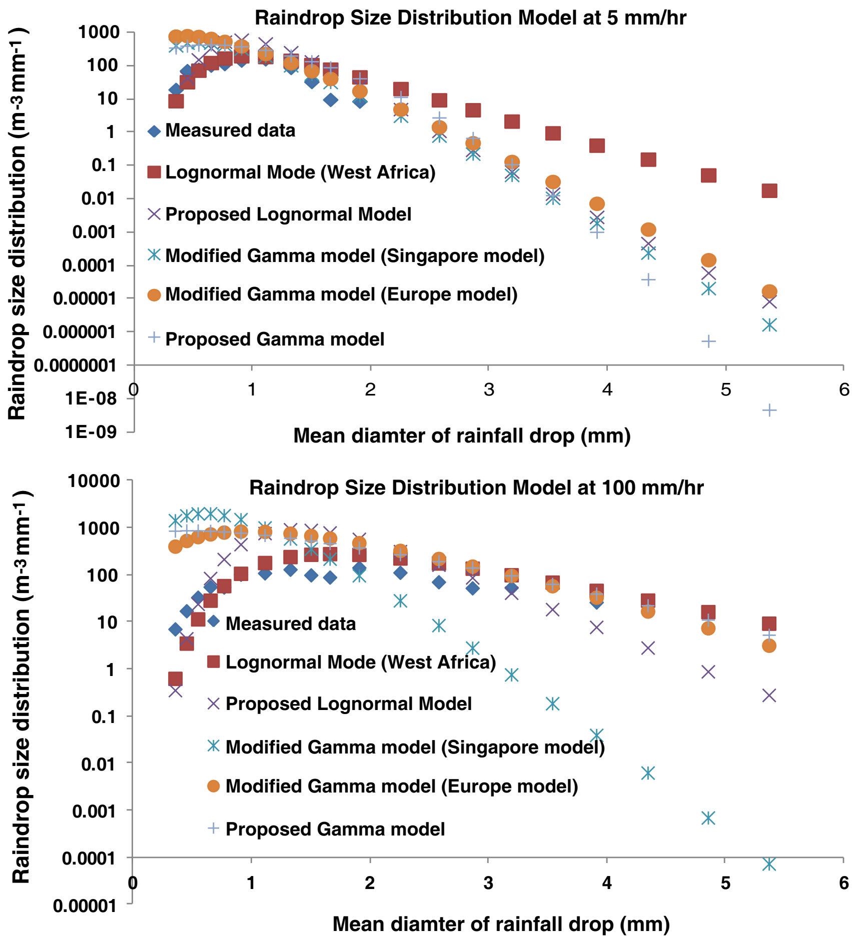

Figure 4. Comparative studies of the proposed model with existing ones at different rain rate.

where Q is the total extinction cross-section in mm^2 which depends on the drop diameter D, wavelength λ, and complex refractive index of the raindrop m. The refractive index of the raindrop also depends on the propagating frequency, temperature and drop size distribution. Q is given as:

$$Q(D, \lambda, m) = \frac{\lambda^2}{2\pi} \text{Re} \sum_{n=1}^{\infty} (2n+1)(a_n + b_n) \tag{18}$$

where Re is the real part of the expression (18), and a_n and b_n are the Mie scattering coefficients which depend on the drop diameter, wavelength and complex refractive index of the raindrops. The complex refractive index is determined by using the Liebe model [40]. The average maximum temperature (28°C) during the summer period (rainy season) in Durban is adopted. Using the general power law, the specific rain attenuation is equivalent to:

$$A_s = aR^b \quad \text{(dB/km)} \tag{19}$$

In order to determine the coefficients a and b, Equations (17) and (18) are used for specific attenuation computations and the results fitted as a function of rainfall rate via the regression technique. The specific attenuation is determined for different rain types by using the Liebe complex refractive index model, the terminal velocity and the different raindrop size distribution model based on rain type regimes. Due to the non-spherical shape of raindrops, a circular polarization is assumed. In order to determine the coefficients for the power law relationship between specific attenuation A_s and rain rate R (mm/hr), the non-linear optimization regression method is used as recommended by ITU-R P.838-3 [42] and the same approach has been employed by several authors [1, 3, 19, 40, 41, 44, 45]. Thus, the coefficients a and b for different rain types are developed considering circular polarization. Table 4 gives a summary of the coefficients with respect to the corresponding rain types. It is noticed that the coefficient a value decreases progressively as the trend moves from drizzle to thunderstorm raindrop regime. In the case of the coefficient b values, the reverse is true. As a function of frequency, as the frequency increases, the coefficient a values increase as well, while the coefficient b values decrease with the increase in frequency in each rain regime.

Figures 5(a), (b), (c), and (d) represent the specific rain attenuation for the drizzle, widespread, shower, thunderstorm and the models compare with the general model derived from the combined rain drop size data, and ITU-R P.838-3 specific rain attenuation for the frequency range 1–100 GHz [42]. It is worth mentioning here that the ITU-R model is based on the Laws-Parsons DSD model, which may not be adequate in a region such as Durban, which is located in the sub-tropical region of the Country.

It is observed from Figure 5 that the specific rain attenuation increases with frequency. The most pronounced specific rain attenuation is recorded in the thunderstorm rain regime while the least value of the specific rain attenuation is found in the drizzle regime.

Considering the frequency of 5 GHz at rain rates of 4 mm/hr, 9 mm/hr, 30 mm/hr and 100 mm/hr, the specific rain attenuation will increase by 67% between the drizzle rain regime and the widespread rain regime. In the case of drizzle and thunderstorm regimes, the increase is approximately 2145%. At the same specified rain rates and frequency of 50 GHz, the drizzle/widespread increase is 69%,

Table 4. Specific rain attenuation power law coefficients for different rain types.

Frequency GHz	Drizzle		Widespread		Shower		Thunderstorm		General	
	a	*b*	*a*	*b*	*a*	*b*	*a*	*b*	*a*	*b*
5	0.0008	0.9679	0.0007	0.9051	0.0004	1.0816	0.0003	1.18	0.00055	1.03365
10	0.0047	1.0554	0.0034	1.1997	0.0026	1.2983	0.0029	1.2661	0.0034	1.2048
15	0.0152	1.1032	0.0127	1.1771	0.0143	1.1396	0.0177	1.0833	0.01497	1.1258
20	0.0333	1.072	0.0287	1.1129	0.0302	1.0989	0.0377	1.0392	0.03247	1.08075
25	0.0591	1.0303	0.0523	1.0376	0.0482	1.069	0.0568	1.0252	0.0541	1.0405
30	0.0937	1.0125	0.086	0.9894	0.0772	1.0296	0.0906	0.9871	0.0868	1.0046
35	0.1368	1.004	0.1302	0.955	0.1196	0.9871	0.143	0.9394	0.1324	0.9713
40	0.1872	0.9934	0.1849	0.9173	0.1709	0.9473	0.2053	0.8984	0.18707	0.9391
50	0.3094	0.9591	0.3373	0.8065	0.2889	0.8621	0.3176	0.8371	0.3133	0.8662
60	0.4665	0.9271	0.5784	0.6811	0.4621	0.7592	0.4363	0.7752	0.4858	0.78565
70	0.6538	0.9086	0.9017	0.5896	0.7272	0.6632	0.6185	0.7072	0.7253	0.71715
80	0.8273	0.9003	1.2113	0.5413	1.0107	0.6028	0.8267	0.6571	0.969	0.67537
90	0.932	0.8967	1.4023	0.5202	1.196	0.5735	0.9659	0.6312	1.12405	0.6554
100	0.9586	0.8954	1.457	0.5122	1.2534	0.5625	1.0071	0.6215	1.169025	0.6479
ITU-R, P.838-3 [42]										
	a (*Horizontal*)	*b* (*Horizontal*)	*a* (*Vertical*)	*b* (*Vertical*)						
5	0.0002162	1.6969	0.0002428	1.5317						
10	0.01217	1.2571	0.01129	1.2156						
15	0.04481	1.1233	0.05008	1.0440						
20	0.09164	1.0568	0.09611	0.9847						
25	0.1571	0.9991	0.1533	0.9491						
30	0.2403	0.9485	0.2291	0.9129						
35	0.3374	0.9047	0.3224	0.8761						
40	0.4431	0.8673	0.4274	0.8421						
50	0.6600	0.8084	0.6472	0.7886						
60	0.8606	0.7656	0.8515	0.7486						
70	1.0315	0.7345	1.0253	0.7215						
80	1.1704	0.7115	1.1668	0.7021						
90	1.2807	0.6944	1.2795	0.6876						
100	1.3671	0.6815	1.3680	0.6765						

while drizzle/thunderstorm increase records approximately 1182%. At 100 GHz, the least % difference is observed for the drizzle/widespread and drizzle/thunderstorm; the values are 35% and 431% respectively. In the case of the general models, the results obtained for drizzle shows about 10% increase in specific attenuation compared to that obtained using the dedicated drizzle model. For rain rates of 9 mm/hr, 30 mm/hr and 100 mm/hr, the specific rain attenuation is less compared to that obtained through the corresponding regime dedicated models for widespread, shower and thunderstorm respectively. Another notable point in Figure 5, is that the ITU-R model overestimated almost in all rain regimes with a less discrepancy at low rain rates. The progressive increase in the differences between the ITU-R model and the proposed models with increased rain rate is an indication of the difference between the proposed DSD models and the Laws-Parsons DSD model.

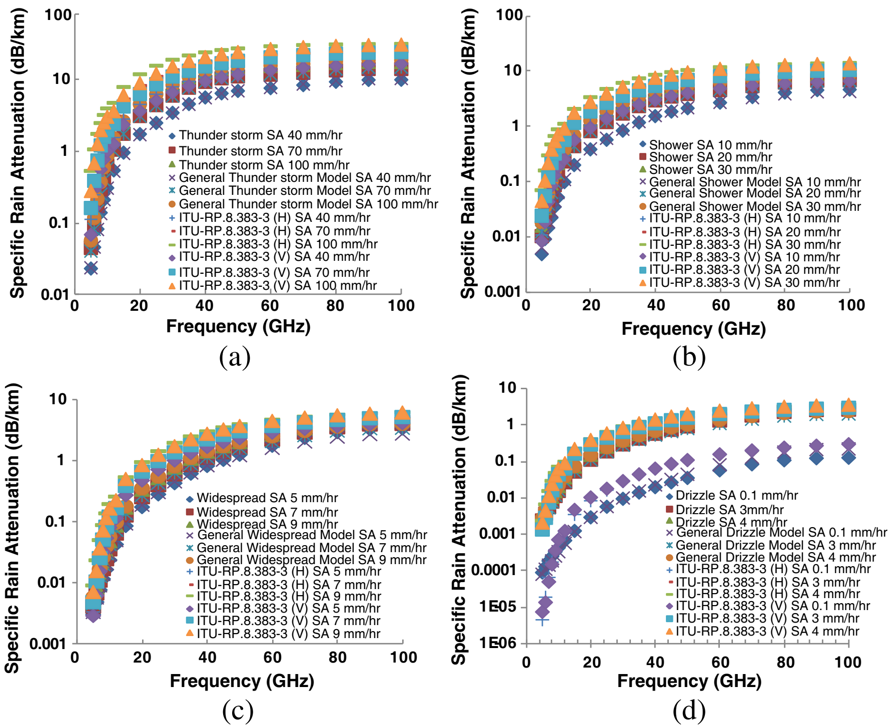

Figure 5. Specific rain attenuation for different rain types and general model.

6. CONCLUSION

In this paper, raindrop size distribution data is modeled using the method of moments and fitted with lognormal and modified gamma distributions. The former is considered because of its average correlation coefficients. The model results are compared with two sub-, and tropical models of West Africa's lognormal and Singapore's modified gamma and lognormal models respectively. The results show that the proposed model performs better at all chosen rain types.

The proposed dropsize models are applied to determine specific rain attenuation coefficients for different rain types and compared to the general model which comprises of all raindrop size distributions. With the exception of the drizzle rain type, the value of the specific rain attenuation obtained using the general model is less compared to the one obtained through their respective dedicated models. The specific rain attenuation for drizzle is 10% higher when employing the general model as opposed to that obtained from the dedicated model. The results of the proposed raindrop size distribution models and specific rain attenuation coefficients may be of great interest to satellite and terrestrial systems designers in Southern Africa.

REFERENCES

1. Ajayi, G. O., S. Feng, S. M. Radicella, and B. M. Reddy, *Handbook on Radio Propagation Related to Satellite Communications in Tropical and Subtropical Countries*, ICTP, 1996.
2. Crane, R. K., *Electromagnetic Wave Propagation through Rain*, John Wiley, 1996.
3. Das, S., A. Maitra, and A. K. Shukla, "Rain attenuation modelling in the 10–100 GHz frequency using drop size distributions for different climate zones in tropical India," *Progress In Electromagnetics Research B*, Vol. 25, 211–224, 2010.
4. Chen, K.-S., C.-Y. Chu, and Y.-C. Tseng, "A semi-empirical model of rain attenuation at Ka-band in Northern Taiwan," *Progress In Electromagnetics Research M*, Vol. 16, 213–223, 2011.
5. Mandeep, J. S. and J. E. Allnut, "Rain attenuation prediction at Ku-band in South East Asia countries," *Progress In Electromagnetics Research*, Vol. 76, 65–74, 2007.
6. Berne, A. and R. Uijlenhoet, "A stochastic model of range profiles of raindrop size distributions: Application to radar attenuation correction," *Geophys. Res. Lett.*, Vol. 32, L10803, 2005, doi:10.1029/2004GL021899.
7. Jameson, A. R. and A. B. Kostinski, "What is a raindrop size distribution?," *Bulletin of the American Meteorological Society*, Vol. 82, 1169–1177, 2001.
8. Owolawi, P. A, "Characteristics of rain at microwave and millimetric bands for terrestrial and satellite links attenuation in South Africa and surrounding islands," Ph.D. Dissertation, School of Electrical, Electronics and Computer Engineering, University of KwaZulu Natal, Durban, South Africa, Jul. 2010.
9. Uijlenhoet, R., J. A. Smith, and M. Steiner, "Microphysical structure of extreme precipitation as inferred from ground-based raindrop spectra," *Journal of the Atmospheric Sciences*, Vol. 60, 1220–1238, 2003.
10. Laws J. O. and D. A. Parsons, "The relation of raindrop-size to intensity," *Trans. Amer. Geophys. Union*, Vol. 24, 452–460, 1943.
11. Marshall, J. S. and W. M. Palmer, "The distribution of raindrops with size," *Journal of Meteorology*, Vol. 5, 165–166, 1948.
12. Quimpo R. G. and A. B. Brohi, "On the frequency distribution of

raindrop sizes," *Journal of Irrigation and Drainage Engineering*, Vol. 112, No. 2, 119–127, May 1986.

13. Owolawi, P. A, "Raindrop size distribution model for the prediction of rain attenuation in Durban," *PIERS Online*, Vol. 7, No. 6, 516–523, 2011.
14. Maaciel, L. R. and M. S. Assis, "Tropical rainfall drop size distribution," *International Journal of Satellite Communications*, Vol. 8, 181–186, 1990.
15. Kumar L. S., Y. H. Lee, and J. T. Ong, "Truncated gamma drop size distribution models for rain attenuation in Singapore," *IEEE Transactions on Antennas and Propagation*, Vol. 58, No. 4, Apr. 2010.
16. Kumar L. S., Y. H. Lee, and J. T. Ong, "Two-parameter gamma drop size distribution models for singapore," *IEEE Transactions on Geoscience and Remote Sensing*, Vol. 549, No. 4, Sep. 2011.
17. Jassal, B. S., A. K. Verma, and L. Singh, "Raindrop size distribution and attenuation for Indian climate," *Indian Journal of Radio and Space Physics*, Vol. 23, No. 3, 193–196, Jun. 1994.
18. Tharek, A. R. and J. Din, "Rainfall drop size distribution measurements in Malaysia," *Proc. URSI Comm. F. 1992 Symposium Wave Propagation and Remote Sensing*, 1.2.1–1.2.5, Ravenscar, North Yorkshire, UK, Jun. 8–12, 1992.
19. Ajayi, G. O. and R. L. Olsen, "Modelling of tropical raindrop size distribution for microwave and millimeter wave applications," *Radio Science*, Vol. 20, 193–202, 1985.
20. Ajayi, G. O. and A. Adimula, "Variations in raindrop size distribution and specific attenuation in a tropical environment," *URSI Comm. F Symposium*, 811–814, La Londe-less Maures, France, Sep. 1989.
21. Sevruk, B. and W. R. Hamon, *International Comparison of National Precipitation Gauges with a Reference Pit Gauge, WMO Instrument and Observing Methods Rep.*, No. 17 111, 1984, [Available from World Meteor. Org., Case Postale 2300, CH-1211, Geneva, Switzerland].
22. Sevruk, B., "Wind induced measurement error for high-intensity rains," *Proc. International Workshop on Precipitation Measurement*, WMO Tech. Document 328, 199–204, 1989, [Available online at http://www.wmo.ch].
23. Groisman, P. Y. and D. R. Legates, "The accuracy of united states precipitation data," *Bull. Amer. Meteor. Soc.*, Vol. 75, 215–227, 1994.

24. Nešpor, V. and B. Sevruk, "Estimation of wind-induced error of rainfall gauge measurements using a numerical simulation," *J. Atmos. Oceanic Technol.*, Vol. 16, 450–464, 1999.
25. Sevruk, B., M. Ondras, and B. Chvila, "The WMO precipitation measurement intercomparisons," *Atmos. Res.*, Vol. 92, 376–380, 2009.
26. Fiser, O., M. Schoenhuber, and P. Pesice, "First results of DSD measurement by video distrometer in the Czech republic in 1998–1999," *Studia Geophysica et Geodetica*, Vol. 46, No. 3, 485–505, 2002.
27. Adimula, I. A. and G. O. Ajayi, "Variation in raindrop size distribution and specific attenuation due to rain in Nigeria," *Ann. Telecom.*, Vol. 51, Nos. 1–2, 87–93, 1996.
28. Timothy, K. I., J. T. Ong, and E. B. L. Choo, "Raindrop size distribution using method of moments for terrestrial and satellite communication applications in Singapore," *IEEE Transactions on Antennas and Propagation*, Vol. 50, 1420–1424, Oct. 2002.
29. Afullo, T. J. O., "Raindrop size distribution modeling for radio link design along the eastern coast of South Africa," *Progress In Electromagnetics Research B*, Vol. 34, 345–366, 2011.
30. Mandeep, J. S. and K. Tanaka, "Effect of atmospheric parameters on satellite links," *Int. Journal Millimeter Wave*, Vol. 28, No. 10, 789–795, 2007.
31. Kumar, L. S., Y. H. Lee, J. X. Yeo, and J. T. Ong, "Tropical rain classification and estimation of rain from Z-R (reflectivity-rain rate) relationships," *Progress In Electromagnetics Research B*, Vol. 32, 107–127, 2011.
32. Gunn, R. and G. D. Kinzer, "The terminal velocity of fall for water droplets in stagnant air," *Journal Atmos. Sci.*, Vol. 6, No. 4, 243–248, 1949.
33. Vivekanandan, J., G. Zhang, and E. Brandes, "Polarimetric radar rain estimators based on constrained gamma drop size distribution model," *J. Appl. Meteorology*, Vol. 43, No. 2, 217–230, 2004.
34. Kozu, T. and K. Nakamura., "Rainfall parameter estimation from dual-radar measurements combining reflectivity profile and path-integrated attenuation," *J. Atmos. Oceanic Tech.*, Vol. 8, No. 2, 259–270, 1991.
35. Ulbrich, C. W., "Natural variation in the analytical form of the raindrop size distribution," *J. Climate Appl. Meteoro.*, Vol. 22, 1764–1775, 1983.
36. Timothy, K. I., S. Sharma, M. Devi, and A. K. Barbara,

"Tropical raindrop size distribution (RDS): Prediction and modeling its effects on microwave propagation," *Proceedings of 9th International Conference on Antennas and Propagation*, 244–248, Eindhoven, The Netherlands, Apr. 4–7, 1995.

37. Pan, W., P. Leung, W. Huang, and W. Liu, "On interval estimation of the coefficient of variation for three-parameter Weibull, lognormal and gamma distribution: A simulation-based approach," *European Journal of Operational Research*, Vol. 164, 367–377, 2005.
38. Ong, J. T. and Y. Y. Shan, "Raindrop size distribution models for Singapore: Comparison with results from different regions," *Proc. 10th Intl. Conf. on Ant. & Prop.*, Vol. 436, 2.281–2.285, 1997.
39. Ong, J. T., K. I. Timothy, T. Kozu, J. W. F. Goddard, J. Eastment, C. Wilson, and J. Tan, "Studies on tropical rainfall structure with RAL S-band radar, TRMM PR and radiosonde-inter comparison," *Proc. — European Geophysical Society, XXVI General Assembly*, France, Mar. 2001.
40. Jiang, H., M. Sano, and M. Sekine, "Weibull raindrop-size distribution and its application to rain attenuation," *IEE Proc., Microwave, Antenna Propagation*, Vol. 144, No. 3, 197–200, Jun. 1997.
41. Yeo, T. S, P. S. Kooi, M. S. Leong, and L. W. Li, "Tropical raindrop size distribution for the prediction of rain attenuation of microwaves in the 10–40 GHz band," *IEEE Transactions on Antennas and Propagation*, Vol. 49, No. 1, 80–82, Jan. 2001.
42. International Telecommunication Union, "Specific attenuation model for rain for use in prediction methods," Recommendation ITU-R, P.838-3, Geneva, 2005.
43. Willmott, C. J. and K. Matsuura., "Advantages of the mean absolute error (MAE) over the root mean square error (RMSE) in assessing average model performance," *Climate Research*, Vol. 30, 79–82, Dec. 2005.
44. Olsen, R., D. Rogers, and D. Hodge, "The aRb relation in the calculation of rain attenuation," *IEEE Transactions on Antennas and Propagation*, Vol. 26, No. 2, 318–329, 1978.
45. Da Silva Mello, L. and M. S. Pontes, "Unified method for the prediction of rain attenuation in satellite and terrestrial links," *Journal of Microwaves, Optoelectronics and Electromagnetic Applications*, Vol. 11, No. 1, Jun. 2012.